# SEPARATING SEPTICEMIC AND NORMAL CHICKEN LIVERS BY VISIBLE/NEAR–INFRARED SPECTROSCOPY AND BACK–PROPAGATION NEURAL NETWORKS

C. Hsieh, Y. R. Chen, B. P. Dey, D. E. Chan

**ABSTRACT.** *The visible/near–infrared spectra of 300 chicken livers were analyzed to explore the feasibility of using spectroscopy to separate septicemic livers from normal livers. Three strategies involving offset, second difference, and functional link methods were applied to preprocess the spectra, while principal component analysis (PCA) was utilized to reduce the input data dimensions. PCA scores were fed into a feed–forward back–propagation neural network for classification. The results showed no obvious difference in classification accuracy between offset and non–offset data when no other preprocessing method was applied. The full 400–2498 nm wavelength region produced better results than the 400–700 nm, 400–1098 nm, and 1102–2498 nm sub–regions when more than 30 PCA scores were used. In general, the classification accuracy was improved by increasing the number of scores of input data, but too many scores diminished performance. The functional link test showed that using functional–link spectra selected at every third point with 60 scores achieved the same classification accuracy as that obtained when using all the data points with 90 scores. The best classification model used offset correction followed by second difference (g = 31) and 60 scores. It achieved a classification accuracy of 98% for normal and 94% for septicemic livers.*

***Keywords***. *Chicken liver, Septicemia, Principal component analysis, Functional link, Classification, NIR spectroscopy, Back–propagation, Neural network.*

With a continually growing demand for poultry products, consumers require more assurance of food safety. The 1968 Wholesome Poultry Products Act requires each poultry carcass sold in the United States to be inspected for its wholesomeness during post–mortem inspection at the poultry processing plant by inspectors from the Food Safety and Inspection Service (FSIS) of the USDA. About 2,200 inspectors (USDA, 2000) are employed to examine the exterior, the inner surfaces of the body cavity, and the organs of each bird for visible abnormalities resulting from diseases. The number of chickens slaughtered at federally inspected establishments increased from 2.8 billion birds in 1965 to 7.5 billion in 1998. In 1998, 78 million birds were condemned because they were diseased and defective. The visual bird–by–bird inspection is labor intensive and prone to human error and variability.

Article was submitted for review in July 2001; approved for publication by the Information & Electrical Technologies Division of ASAE in December 2001.

Mention of company or trade names is for purpose of description only and does not imply endorsement by the USDA.

The authors are **Ching–Lu Hsieh**, **ASAE Member Engineer**, Visiting Scientist, **Yud–Ren Chen**, **ASAE Member Engineer**, Research Leader, and **Diane E. Chan**, Agricultural Engineer, Instrumentation and Sensing Laboratory, USDA Agricultural Research Service, Beltsville, Maryland; and **Bhabani P. Dey**, Veterinary Medical Officer, Animal and Egg Production Food Safety, USDA Food Safety and Inspection Service, Washington, D.C. **Corresponding author**: Yud–Ren Chen, ISL, USDA–ARS, Building 303, BARC–East, 10300 Baltimore Avenue, Beltsville, MD 20705–2350, phone: 301–504–8450; fax: 301–504–9466; e–mail: cheny@ba.ars.usda.gov.

There are six major defects that cause chicken carcasses to be removed from the processing line. They are septicemia, cadaver, bruise, tumor, airsacculitis, and ascites. Under the current HACCP–based Inspection Models Project (HIMP), FSIS requires that any poultry showing evidence of septicemia, which is a systemic condition and a manifestation of infectious disease caused by pathogenic microorganisms in the blood, shall be condemned (zero tolerance) (Chen et al., 2001).

Near–infrared (NIR) spectroscopy has proven its value in food quality inspection for several reasons. For instance, it is a rapid, non–invasive, and reliable method. Osborne et al. (1993) reported that applications of NIR spectroscopy in food and beverage analysis could categorize constituents including moisture, protein, fat, and carbohydrate content. NIR spectra (700–2500 nm) of food constituents show overlapping bands, which correspond mainly to overtones and combinations involving chemical bonds in molecular vibration. For example, the carbon–hydrogen (C–H) bond shows first and second overtones at 1765 nm and 1215 nm for the $CH_2$ structure (Osborne et al., 1993). Different compounds demonstrate overtones and combinations of bond vibrations in different wavelength regions. In the visible region (400–700 nm), spectral absorption is due to electronic transition. It is closely related to the color pigments of the sample. In NIR applications, the reflected signal contains information about the composition of the testing sample because the diffuse reflectance of the sample is determined by the absorption properties of its major chemical constituents and by its physical light–scattering properties (Norris, 1989). The Instrumentation and Sensing Laboratory (ISL) of the USDA has developed a visible/near–infrared (Vis/NIR)

system to measure spectral characteristics of agricultural products in both the visible light and NIR regions. This system has been shown feasible for chicken carcass inspection, and on–line trials have been conducted (Chen and Massie, 1993; Chen et al., 1998; Chen et al., 2000; Park et al., 1995).

NIR analysis usually requires knowledge of the chemical composition of a calibration set of samples. The relationship between chemical and spectral data is generally created by multivariate linear regression. Principal Component Analysis (PCA), a multivariate analysis method based on eigenvector models, can resolve the problem of correlation between wavelengths, reduce the spectra to a small number of linearly independent values, and provide information as to the nature of underlying chemical factors affecting variation in the spectra (Cowe and McNicol, 1985). Devaux et al. (1986) reduced spectral patterns from 351 wavelengths to 10 independent variables using PCA with enough information for discriminating bread–baking quality of wheats. Chen et al. (1998) utilized PCA to reduce the input variables from 190 to 15 variables and successfully classified normal and abnormal chicken carcasses.

In quality prediction or classification of agricultural products, models using neural networks have been reported that are more robust than those using some other statistical methods (i.e., Bayesian statistical classifiers or multivariate linear regression). Conventional statistical methods are limited when the parameters are too many or the statistical properties of the classes are unknown or cannot be estimated (Gonzalez and Woods, 1993; Thai and Shewfelt, 1991). Næs et al. (1993) compared back–propagation neural network models with partial least squares and principal component regression in prediction. They found that neural networks gave more accurate prediction. Brons et al. (1991) showed that statistical methods increased neural network efficiency when they were applied as preprocessors to the data before building the neural network. Because a neural network contains many advantages, including nonlinear, adaptive, and parallel processing, it was found to have many successful applications in classification, recognition, pattern completion, and optimization (Kung, 1993). Many research studies have been published. Among them, Park et al. (1994) applied a back–propagation model to classify beef sensory attributes using ultrasonic spectral feature as input data. Hsieh et al. (1997) classified head cabbage seedlings at five different stages by applied a four–layer back–propagation model with image texture analysis techniques. An application of the back–propagation model has been explored and tested on–line using the Vis/NIR spectrum for separating normal and abnormal poultry carcasses (Chen et al., 1998).

The Vis/NIR spectroscopy system developed by ISL has been found capable of on–line chicken carcass classification. However, the system is limited to examining carcasses. In addition, procedures that only scan or image the carcass exteriors are different from the whole–bird inspection performed by the inspectors and may not detect some condemned conditions. Thus, there is a need to acquire additional feature information from post–mortem poultry at different positions (e.g., body cavity) and/or from different internal organs (e.g., liver and heart). A study on chicken viscera has been reported by Chao et al. (1999). A neuro–fuzzy–based color imaging system was used to classify poultry viscera into normal, airsacculitic, cadaver, and septicemic categories.

Since the presence of any septicemic condition is due to some kind of infectious disease affecting the entire body of the bird, a diseased chicken with septicemia will have an abnormal liver. The object of this current research was to study the feasibility of applying a Vis/NIR technique to separate septicemic chicken livers from normal livers. Data preprocessing methods including offset, second difference, and functional link, and a dimensionality reduction measure (PCA) applied to a back–propagation neural network were compared. These methods were examined with the intent of expanding the application of Vis/NIR system for the inspection of organs along with the chicken carcass so that the classification accuracy can be improved.

## Materials and Methods

### Sample Preparation

A total of 300 chicken livers, 150 normal and 150 septicemic, were collected from poultry processing plants on the eastern shore of Maryland from August 2000 to March 2001 (shown in table 1). Chickens were inspected and assigned to normal or septicemic classes by FSIS veterinarians. Before collecting livers from birds found to be normal or birds condemned due to septicemia, the general body condition of the bird and the color and condition of the liver, gall bladder, spleen, heart, lungs, muscle, and skin were noted. For each bird, the organs were collected and stored in a new, sealable plastic bag. The bagged organs were preserved in a cooler filled with ice and brought back to the laboratory within 2–3 hours. Collected in the morning, the samples were prepared for spectral measurements in the afternoon. A 4 cm diameter core cutter was used to cut a circular piece from each liver. The piece was fitted inside a cylindrical sample cup with top surface of the liver against the sample window. Spectra were measured using an NIRSystems model 6500 scanning monochromator (Silver Spring, Md.). The computer automatically converted reflectance values to absorbance values, i.e., log(1/R). Each 1050–point spectrum was an average of 32 scans, collected over the 400–2498 nm wavelength range at 2 nm intervals.

To reduce the effect of possible variation due to different growers, growing season, etc., the training and testing data set were randomly chosen on each sampling date (shown in table 1). From a total of 300 samples, 200 were used for training and 100 for testing.

### Data Preprocessing

Figure 1 shows a flowchart of the data preprocessing and classification schemes applied in this study. Three preprocessing strategies were applied to enhance different features of the spectral data. In strategy I, an offset correction was applied and followed by PCA to reduce the number of variables. In strategy II, offset correction and second difference were used before PCA. In strategy III, offset correction, second difference, and functional link were implemented before PCA. The spectral data were enhanced by different data preprocessing strategies, and the PCA scores were input to a back–propagation neural network for classification. The classification results were then compared.

**Table 1. Dates and numbers of samples collected and randomly selected for training and testing sets.**

| | Collected | | Training Set | | Testing Set | |
|---|---|---|---|---|---|---|
| Date | Normal | Septicemic | Normal | Septicemic | Normal | Septicemic |
| 31 Aug 2000 | 5 | 13 | 3 | 8 | 2 | 5 |
| 7 Sep 2000 | 6 | 14 | 4 | 9 | 2 | 5 |
| 27 Sep 2000 | 4 | 15 | 3 | 10 | 1 | 5 |
| 5 Oct 2000 | 3 | 10 | 2 | 7 | 1 | 3 |
| 6 Oct 2000 | 7 | 10 | 5 | 7 | 2 | 3 |
| 6 Dec 2000 | 30 | — | 20 | — | 10 | — |
| 7 Dec 2000 | 30 | — | 20 | — | 10 | — |
| 12 Dec 2000 | 16 | 17 | 10 | 11 | 6 | 6 |
| 25 Jan 2001 | 6 | 20 | 4 | 13 | 2 | 7 |
| 1 Feb 2001 | 14 | 12 | 9 | 8 | 5 | 4 |
| 8 Feb 2001 | 15 | 10 | 10 | 7 | 5 | 3 |
| 7 Mar 2001 | 14 | 29 | 10 | 20 | 4 | 9 |
| Total | 150 | 150 | 100 | 100 | 50 | 50 |

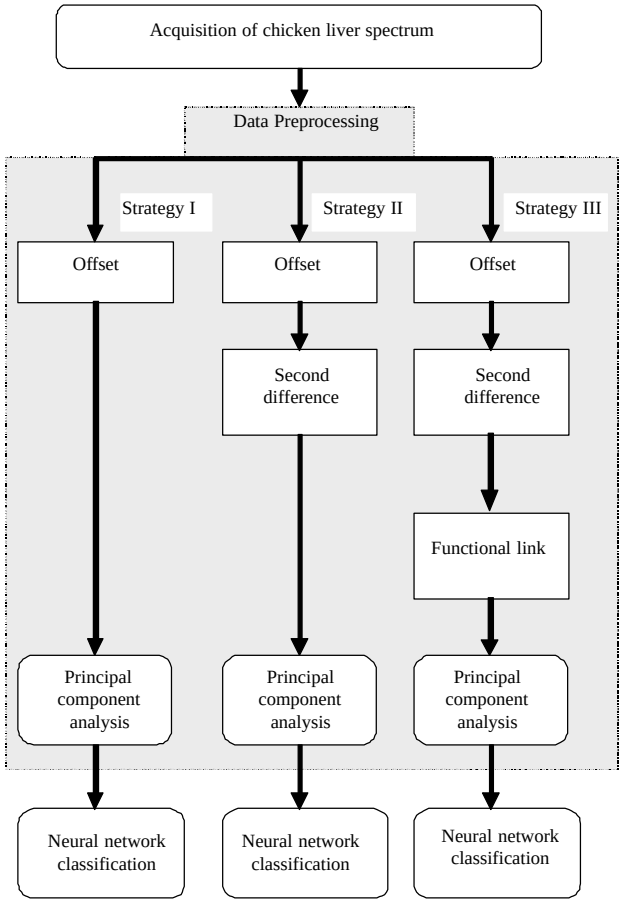


**Figure 1. Flowchart of chicken liver classification.**

### *Offset Correction*

Offset correction usually is applied to eliminate the scattering or distance effects (Hruschka, 1987) on spectra applications. The algorithm used in this study sets the spectra to the same baseline by adding or subtracting a constant (offset) at each point in a spectrum to move its minimum absorption value to zero. The offset correction can be formulated as:

$$S^0_n = S_n - C \quad (1)$$

where

$S^0_n$ = spectral value at the $n$th point after offset
$S_n$ = spectral value before offset
$C$ = offset constant for all points of a particular spectrum.

Offset preprocessing was performed using GRAMS/32 (Galactic Industries Corporation, 1999) spectral processing software.

### *Second Difference*

The second difference method is commonly used in spectroscopy data analysis to separate overlapping spectra and remove baseline shifts (Hruschka, 1987). A reflectance spectrum shows absorbance features directly, while the second difference method extracts the curvature properties of the reflectance spectrum. The finite–difference method used here requires gap size as a parameter for calculating the difference points. Usually measured in wavelength span or data points, different gap sizes extract different curvature properties. Here, the second difference is defined as:

$$S''_n = S_{n+g} - 2 \times S_n + S_{n-g} \quad (2)$$

where $S_n$ is the spectral value at the $n$th point, and $g$ is the gap size in data points. In this study, $g$ was evaluated at values of 2, 8, 15, 31, and 75 data points, based on a previous study. FLMK, a FORTRAN–based program developed by ISL, was used in second difference preprocessing.

### *Functional Link*

Functional–link networks were introduced by Pao in 1989. The main idea of the method is to find a suitably enhanced representation of the input data to generate the higher effects and artificially increase the dimension of the input space (Zurada, 1992). Thus, functional link input data is a combination of the original input pattern and the enhanced input pattern. A block diagram of a functional link network is shown in figure 2. The enhanced pattern is generated by a linearly independent function or formulation from the original pattern components. By extending the dimensionality of the input space, the linearly nonseparable patterns can be separated. In this research, the offset–corrected spectrum ($O_i$) was enhanced using a second difference calculation, and this enhanced spectrum ($H_i$) was then combined with the offset–corrected spectrum to form a

functional link input pattern. For a single functional link input pattern ($F_i$), the formula is:

$$F_i = O_i \mid H_i \tag{3a}$$

where | symbolizes the appending of $H_i$ to $O_i$. $F_i$ has length $q = p + d$, where $p$ is the number of data points in $O_i$, and $d$ is the number of data points in $H_i$. The number of data points varies with the strategy applied. In a matrix form, the equation is:

$$\mathrm{F} = \mathrm{O} \mid \mathrm{H} \tag{3b}$$

where F is the set of functional link input data vectors of size $n \times q$, where $n$ is the number of samples used. O and H have dimensions $n \times p$ and $n \times d$, respectively.

### *Principal Component Analysis (PCA)*

PCA approximates the spectral vector ($A_i$) with a linear combination of a set of orthogonal (uncorrelated) factors ($F_j$), also known as eigenvectors or loadings:

$$A_i \cong s_1F_1 + s_2F_2 + s_3F_3 + ...s_kF_k \tag{4}$$

where the coefficients $s_k$ are called scores. The number of factors used ($k$) depends on the strategy applied. In matrix form, the approximation is:

$$\mathrm{A} \cong \mathrm{S} \times \mathrm{F} \tag{5}$$

where

A = offset–corrected, second difference, or functionally linked spectral matrix
S = PCA score matrix
F = PCA factor matrix.

A, S, and F have dimensions $n \times q$, $n \times k$, and $k \times q$, respectively. In this study, the parameter $k$ was evaluated at 5, 15, 30, 60, and 90; $n$ = 200 for the training set and $n$ = 100 for the testing set; and $q$, the number of data points in a spectrum trace, varied depending on strategy.

The first factor, a vector of spectral reflectance, is chosen to account for the largest possible variance of reflectance in the class. Each successive factor is then chosen to account for the largest possible amount of the remaining variance. Each spectrum can be adequately represented by a few factors in factor space instead of many reflectances in wavelength space. In this way, the dimension of the spectra in wavelength space can be transformed into a vector space with $k$ dimensions spanned by $k$ factors (Galactic Industries Corporation, 1999; Pimentel, 1979).

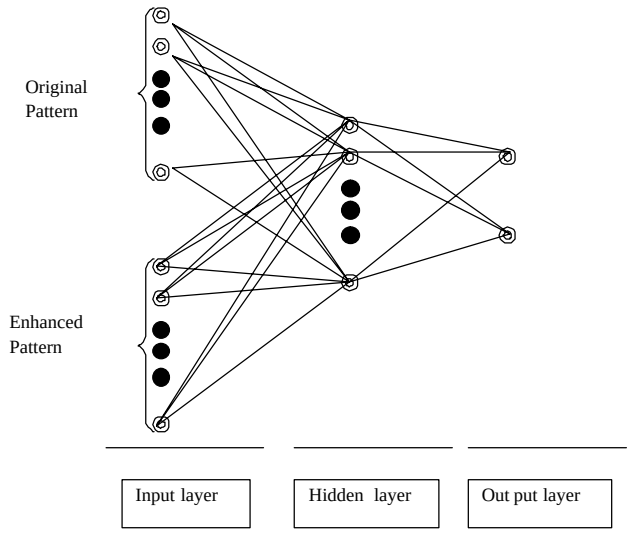


**Figure 2. Block diagram of functional link network.**

The PRINCOMP procedure and the SCORE procedure in the SAS software (SAS, 1999) were employed to form the factors and scores in the PCA process. Normal chicken livers for the training set were used to generate the PCA factors by the PRINCOMP procedure. Based on these factors, the scores were computed by the SCORE procedure for the normal training and testing sets and for the septicemic training and testing sets, respectively. The basic assumption of this PCA application was that the normal chicken liver spectra were better defined as a class in the factor space. Any scores formed from these normal chicken liver factors will fall into the normal group if they have the same score features as the normal livers. Otherwise, they do not belong to the normal group and should be assigned to the septicemic group.

### Back–Propagation Neural Network

A feed–forward back–propagation neural network is a supervised neural network. It consists of an input layer, one or several hidden layers, and an output layer. For a linear application, no hidden layer is necessary. Too many or too few hidden layers or hidden nodes can cause an effect of overfitting or underfitting (Næs et al., 1993). Haykin (1994) summarized the algorithm of feed–forward back–propagation in five steps: (1) start with a reasonable network configuration and set all weights of the network to small random numbers, (2) present the network with training examples, (3) compute the activation potentials and function signals of the network by proceeding forward through the network, (4) compute the gradients of the network by proceeding backward and adjusting weights of the network in each layer according to the learning–rate parameter and momentum constant, and (5) iterate the computation until the network stabilizes or the error is at a minimum or acceptably small value.

The back–propagation element transforming its inputs could be formulated as (NeuralWare, 1998):

$$\begin{aligned} x_j^{[s]} &= f\left\{\sum\left(w_{ji}^{[s]} \times x_i^{[s-1]}\right)\right\} \\ &= f\left(I_j^{[s]}\right) \end{aligned} \tag{6}$$

where

$f$ = nonlinear transfer function. For example, the sigmoid function is defined as:

$$f(z) = \frac{1}{1.0 + e^{-z}} \tag{7}$$

$x_j^{[s]}$ = current state of $j$th neuron in layer $s$

$w_{ji}^{[s]}$ = weight on connection joining $i$th neuron in layer $(s - 1)$ to $j$th neuron in layer $s$

$I_j^{[s]}$ = weighted summation of inputs to $j$th neuron in layer $s$.

During the learning phase, the training vectors from the training sample set were presented to input nodes. If the output pattern did not match the pattern of the classes of the

attributes, the weights in the net were adjusted by a gradient descent rule as follows:

$$\Delta w_{ji}^{[s]} = l_{cof} \times e_j^{[s]} \times x_i^{[s-1]} + \alpha \Delta w_{ji}^{[s-1]} \quad (8)$$

where

$l_{cof}$ = learning coefficient
$\alpha$ = momentum
$e_j^{[s]}$ = error of $j$th neuron in layer $s$.
The error $e_j^{[s]}$ is formulated as follows:

$$e_j^{[s]} = x_j^{[s]} \times \left(1.0 - x_j^{[s]}\right) \times \sum_k \left(e_k^{[s+1]} \times w_{kj}^{[s+1]}\right) \quad (9)$$

By iteratively propagating the error back from the output layer to the previous layer, the neural network system adjusted its weights to minimize the root mean square (RMS) error between desired and actual network outputs.

NeuralWorks Professional II/Plus software (NeuralWare, 1998) with the delta learning rule and sigmoid transfer function was used. A "Savebest" feature of NeuralWorks software was used to optimize training. With this function, the training model is used to predict the testing set after every 100 iterations of the training cycle. If the model shows improvement in terms of predicting the testing set, it is saved, so that the "best" weights are those resulting in the best prediction of the testing set during the total training of 100,000 iterations. The momentum function in NeuralWorks software was also enabled to improve the learning process. The momentum is set to 0.4 by default.

The back–propagation neural network model employed in this study for classification consists of one input layer, one hidden layer, one output layer, and one bias node. The input nodes are the scores obtained from PCA after preprocessing, while the two output nodes indicate normal and septicemic classes. Nodes in the hidden layer are varied according to the number of input nodes, numbering roughly equal to half of the input nodes. Thus, the neural structures in input–hidden–output nodes for this study are 5–3–2, 15–7–2, 30–15–2, 60–30–2, and 90–45–2.

## Results and Discussion

### Pathology of Sample Chicken Livers

The post–mortem examination of each bird for its general condition; the size, color and texture of the carcass; and the gross appearance of the liver, gall bladder, spleen, heart, and lungs was performed by the plant veterinarian. For the normal birds, carcass weight ranged between 1.8 kg and 2.3 kg, and their color had a uniform yellowish tinge. The color of the livers from the normal birds varied more, ranging from light brown to deep brown, chocolate brown, and even magenta for some. However, they generally were smooth with a firm texture, and varied in size from 7.6 × 5.1 cm to 8.9 × 6.3 cm.

For the septicemic birds, abnormal changes in condition were noted primarily in the liver, gall bladder, spleen, heart, and lungs. Some of the septicemic livers presented only one notable change. However, many livers showed multiple changes. The numbers of samples displaying these conditions were as follows: 37 congestion, 81 enlargement, 30 hemorrhage, 1 cyanosis, 12 necrosis, 2 mottled, 50 pliable or fragile, 1 pulpy or gritty texture, and 17 covered with gelatinous material or a membrane. The septicemic livers showed colors ranging from oxblood to blue to black. Histopathological tests of a subset of the samples (99 liver samples with 28 normal and 71 septicemic) were also conducted. All 28 normal livers were identified to be without pathological syndrome. All 71 septicemic liver samples were identified by microscopic examination as having pathological changes in the liver tissue.

Table 2 summarizes the testing models examined in this article. There were 20 testing models: 13 for input data preprocessing, five for dimensionality reduction, and two for neural network training strategy.

### Strategy I

Figure 3 shows the average spectra of 150 normal and 150 septicemic chicken livers with offset and non–offset correction. The GRAMS offset function found that the minimum log(1/R) value occurred at 1100 nm. Each absorption spectrum was adjusted relative to this point automatically by applying the GRAMS offset function. The discontinuity at the 1100 nm offset point is caused by the change between two detectors in the NIRSystems 6500: a silicon detector for 400–1098 nm region, and a lead sulfide detector for the 1100–2498 nm region. A higher log(1/R) value indicates that more radiation has been absorbed (less reflected) by the sample at the corresponding wavelength. In figure 3, four apparent differences between averaged normal and septicemic spectra were indicated in the 600–1000 nm, 1100–1400 nm, 1400–1900 nm, and 1900–2498 nm regions. These shifts in absorbance implied that differences between normal and septicemic livers spectra existed in these regions.

Figure 4 shows the classification accuracy (percentage of correctly classified samples in the testing set) when using full–range (400–2498 nm) offset and non–offset spectra with PCA and neural network classification. It is evident that higher accuracy can be expected with the use of more scores, which include more details from each spectrum. The highest accuracy resulted from using 90 scores for both offset and non–offset spectra. Figure 4 also shows that a minimum number of scores are required when high accuracy is desired. For instance, at least 15 scores are necessary to obtain 80% accuracy. No difference in the classification accuracies for offset and non–offset treatment was observed, except for the 30–score model, in which case offset performed better by 3%. Although no significant difference results from offset correction when classifying chicken livers using spectra

**Table 2. List of testing models in chicken liver classification.**

| Testing Target | Testing Strategy | Testing Model |
|---|---|---|
| Data pre–processing | Offset correction | Offset:<br>400–700 nm<br>400–1098 nm<br>1102–2498 nm<br>400–2498 nm<br>and non–offset. |
| | Second difference (gaps) | 75, 31, 15, 8, 2 points. |
| | Functional link (data points) | All, every third, and every fifth. |
| Dimension reduction | PCA (number of scores) | 5, 15, 30, 60, and 90. |
| Classification | Neural network | Iteration and momentum. |

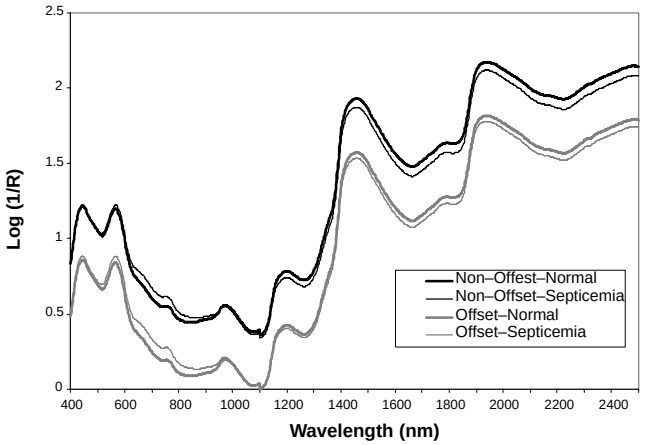


**Figure 3. Average spectra of 150 normal and 150 septicemic chicken livers with/without offset correction.**

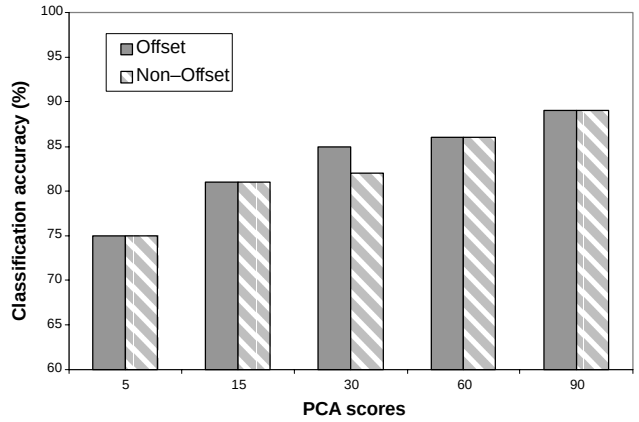


**Figure 4. Comparison of classification accuracy for offset and non–offset chicken liver spectra with various scores.**

given no other preprocessing treatment, offset correction is still recommended since it reduces the scattering or distance effect that, under other conditions, cannot always be controlled.

### Wavelength Region

Figure 5 shows the classification accuracy when using spectral data from different wavelength regions. The performance of the 400–1098 nm region was better than that of the more limited 400–700 nm and 1102–2498 nm regions when more than 30 PCA scores were used. This suggests that using both color and chemical compound information should generally improve chicken liver classification. The four areas containing shifts in absorbance between normal and septicemic spectra shown in figure 3 also support this. In these wavelength region tests, increasing the numbers of scores does not necessarily improve the classification accuracy. For example, the 400–700 nm and 400–1098 nm regions both show highest accuracy with 15 scores, and the 1102–2498 nm regions with 60 scores. This may indicate that too many scores will diminish performance if the original input data points are limited, since the extra scores may contain more noise than useful information. Figure 5 shows that the highest classification accuracy was found with 90 scores in the 400–2498 nm range, which includes colors and chemical reflectance properties.

### Strategy II

Figure 6 depicts a liver spectrum after second difference preprocessing using the finite–difference method with gaps of varying size. The gaps function like band filters, extracting different features from the original spectrum trace. Small gaps are like high–pass filters, while large gaps are low–pass filters. It is important to select an appropriate gap size to extract representative features. If the gaps are too small, important information will be poorly extracted from among other features, but if the gaps are too large, information will be smoothed out, and finer variations in the spectra will be lost. The gap size also affects the processed spectrum trace length. For example, for a spectrum processed with a second difference gap of 15 points, the second difference spectrum will lose its first and last 15 points of original spectrum. If there is a discontinuity in the original spectrum, such as the 1100 nm offset correction point in the liver data, then the points around the discontinuity should be omitted when using the second difference spectrum. The larger the gap size, the more points will be removed from the processed spectrum. Even more points may be lost if other preprocessing is applied before the second difference (e.g., a 4–point running mean smooth would remove 4 points from each end of the spectrum).

Figure 7 shows the classification accuracy from using full–range (400–2498 nm) second difference spectra with gaps of 2, 8, 15, 31, and 75 points. The gap of 31 points with 60 scores gave the highest classification accuracy. The gaps of 15 and 31 generally performed better than the others. The second difference spectra with gaps of 8, 31, and 75 points showed optimal classification with 60 scores, while gaps of 2 and 15 performed best with 90 scores.

### Strategy III

Three functional link spectra generated by taking an offset–corrected spectrum and appending to it its corresponding second difference spectrum (using g = 15, 31, and 75) are shown in figure 8A. Reduced spectra, created by taking every third (one–third) and every fifth (one–fifth) data point of a functional link spectrum are shown in figures 8B and 8C, respectively. As illustrated, there are no significant changes in spectrum shape, and the original traces are reduced to one–third and one–fifth of their original length.

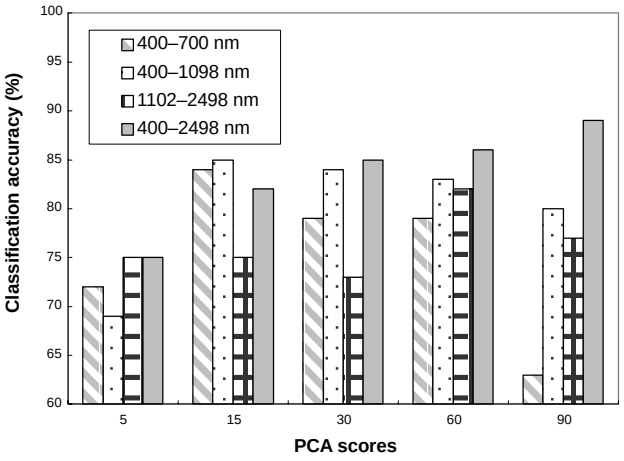


**Figure 5. Comparison of classification accuracy on different wavelength regions with various scores.**

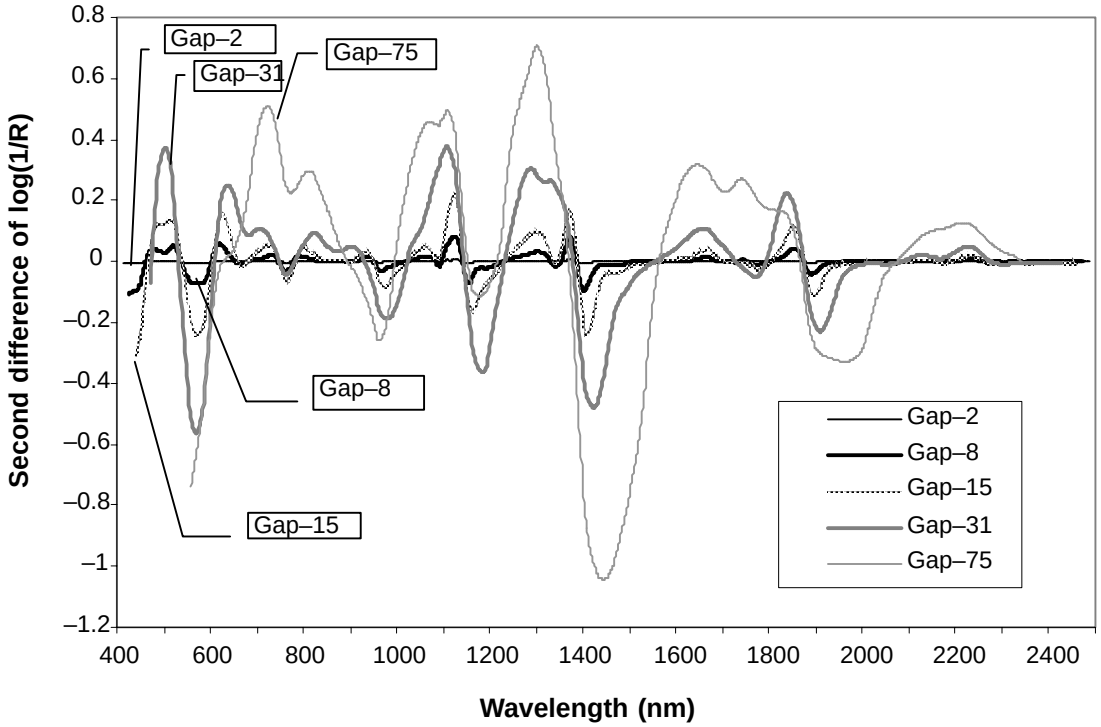


**Figure 6. Spectrum trace after second difference processing with various gaps.**

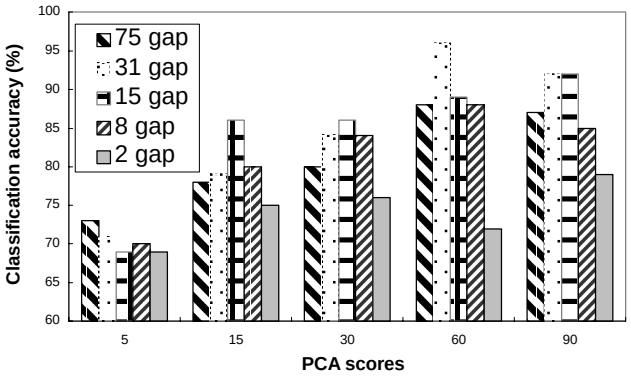


**Figure 7. Comparison of classification accuracy for various second difference gaps in 400–2498 nm wavelength region.**

Table 3 shows the classification accuracies for data preprocessing strategy III followed by the neural network. Both the full spectra used with 90 scores (g = 15 or 75) and one–third spectra used with 60 scores (g = 15) were able to achieve 92% accuracy. Because the model with every third data point requires fewer scores to perform with similar accuracy to the full–spectral model with more scores, the model with every third data point was considered the best model among the functional link models. This also suggests that, with appropriate preprocessing choices, reducing the number of input data points and scores need not diminish performance.

### Number of Training Iterations and Momentum of Neural Network

In the application of a neural network, the number of training iterations is an important factor affecting the model robustness. Overtraining and undertraining will occur when training iterations are too many or too few. Besides training iterations, momentum also contributes to improving the learning speed with a low learning coefficient. A model from strategy II with offset preprocessing followed by second difference (g = 31) and 60 input scores was chosen for this test. In this test the "Savebest" feature of NeuralWorks software was disabled to obtain the classification accuracy at desired iterations. Figures 9A, 9B, and 9C show the classification accuracy as affected by iterations when momentum is set to 0.2, 0.4, and 0.8 respectively. With fewer than 40,000 iterations in an undertrained model, classification accuracy is lower in all three cases. But when 90,000 iterations are exceeded, the classification accuracy also decreases slightly in all three cases. Thus, proper training falls between 40,000 and 90,000 iterations.

These figures also show that lower momentum gives more consistent training and testing results than high momentum. Training and testing accuracies are similar in figure 9A with lower momentum, whereas in figure 9C the higher momentum resulted in overfitting and a testing accuracy that fell further below training accuracy. For example, after 90,000 iterations, 99% training accuracy could be reached, but the corresponding testing accuracy was only 93%. ). Thus, using smaller momentum (e.g., 0.2 or 0.4) could obtain a more consistent result between training and testing; on the contrary, using larger momentum (e.g., 0.8) would tend to result in an overfitting model.

### Optimum Model

Table 4 summarizes the classification accuracy of the optimum models obtained from data preprocessing strategies I, II, and III and the neural network. Offset preprocessing with 90 scores is the optimum model for strategy I. Offset preprocessing followed by second difference (g = 31) and 60 input scores is the optimum model for strategy II. One–third reduced functional link spectra, combining offset

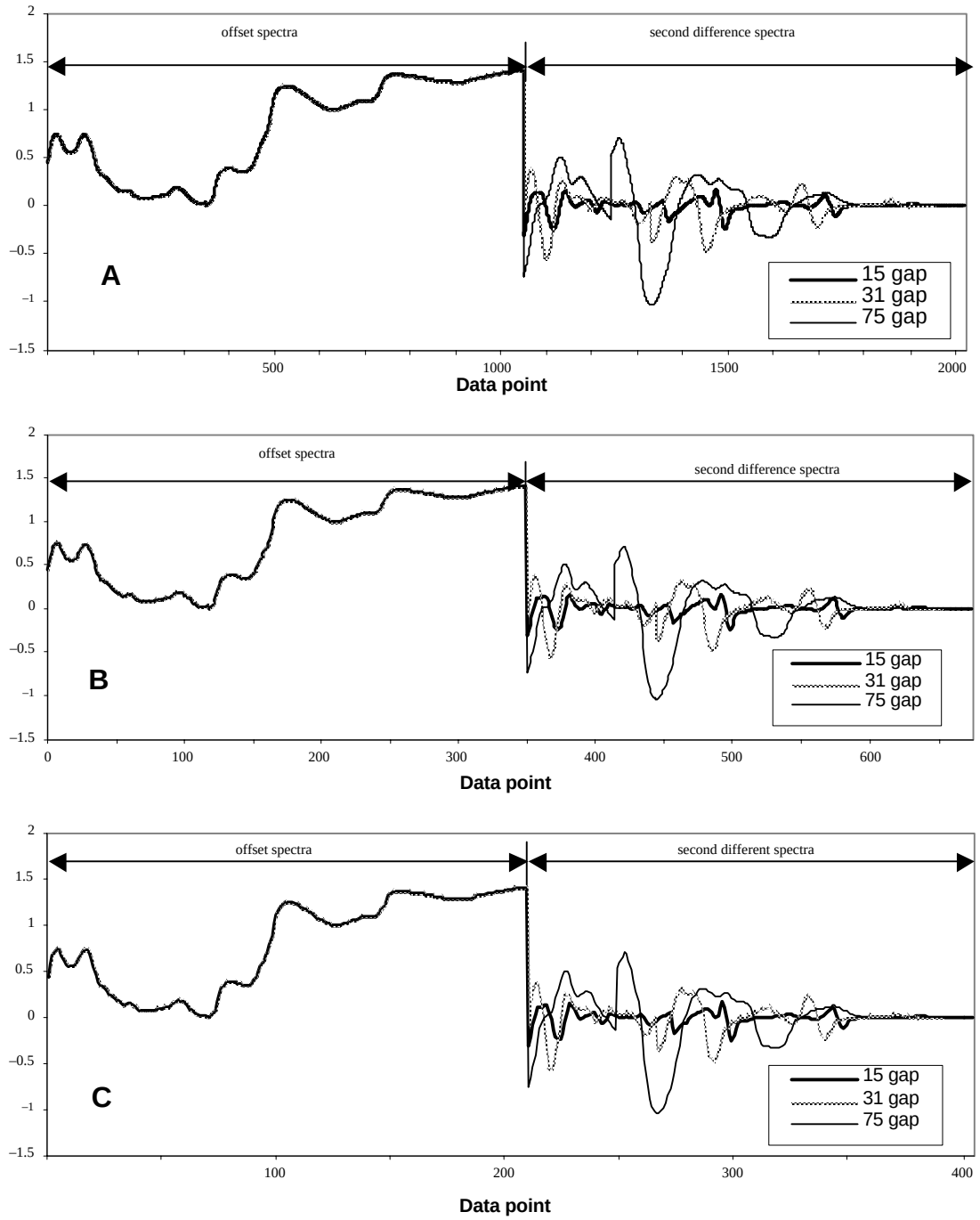


**Figure 8. One example of functional link spectra: A = all data points, B = every third data point, and C = every fifth data point.**

**Table 3. Classification accuracy of functional link models.**

| | | Score | | | | |
|---|---|---|---|---|---|---|
| Data Point | Gap | 5 | 15 | 30 | 60 | 90 |
| All | 15 | 75 | 84 | 84 | 91 | 92 |
| | 31 | 77 | 81 | 83 | 88 | 87 |
| | 75 | 75 | 82 | 83 | 91 | 92 |
| Every third | 15 | 75 | 84 | 83 | 92 | 85 |
| | 31 | 76 | 82 | 84 | 89 | 89 |
| | 75 | 75 | 82 | 84 | 89 | 89 |
| Every fifth | 15 | 75 | 85 | 85 | 90 | 88 |
| | 31 | 76 | 82 | 86 | 86 | 86 |
| | 75 | 75 | 82 | 83 | 87 | 89 |

and second difference (g = 15) data, with 60 input scores, is the optimum model for strategy III. Among these three optimal models, strategy II was the best classification model, with 98% and 94% classification accuracy for normal and septicemic livers, respectively.

The classification accuracies of strategy III (92% for both normal and septicemic) fell below those of strategy II (98% normal, 94% septicemic). This may be the result of enlarging the input data dimension by using the functional link spectra in strategy III, where 90 scores may simply not have been enough to extract all the useful information because the training set of 100 samples limits the maximum number of scores and factors that can be calculated by PCA. More samples may be necessary to optimize the functional link

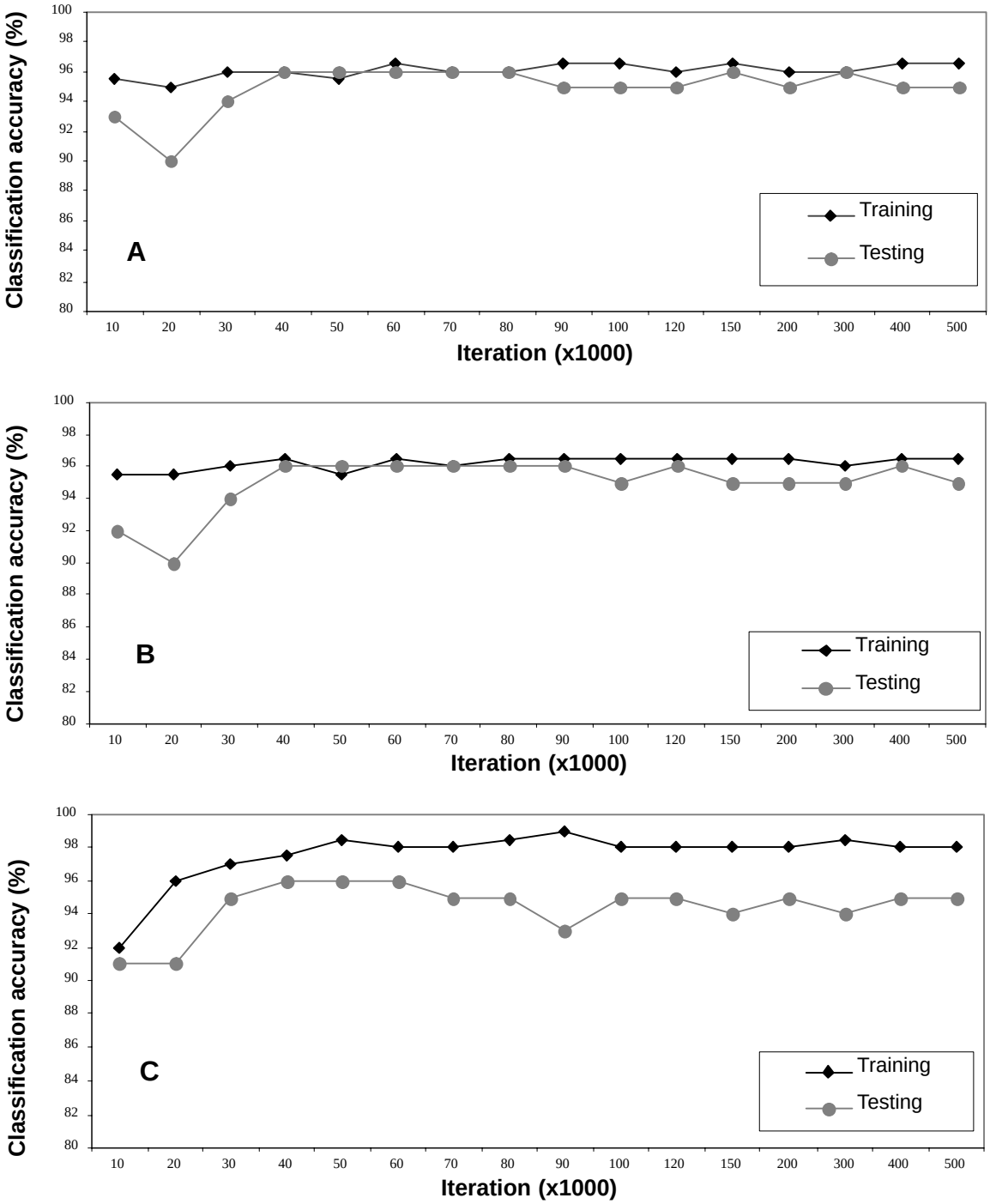


**Figure 9. Momentum and iteration effects on classification accuracy for training and testing: (A) momentum = 0.2, (B) momentum = 0.4, and (C) momentum = 0.8.**

approach. Strategy III performed 6% better than strategy I in classifying the spectra of septicemic livers, which implies that the combined spectral intensity and curvature information is more useful than the intensity information alone.

Table 5 lists misclassified samples for optimum model in strategies I and II. It shows that strategy II reduced the misclassified samples from 19 to 10, an improvement approximately 47.4%. This demonstrates that the second difference is a useful method in chicken liver classification. Among the misclassified samples, normal sample N102 and N119 were always misclassified in the training and testing process, respectively, regardless of the strategy used. Repeated misclassification also occurred to septicemic samples S237, S734, and S738 in training and S268 in testing. One possible reason is that because the veterinarians judged the livers based on the physical condition of the birds, some birds that were small in size but had normal livers may have been inappropriately assigned to the septicemic group. Similarly, some birds without any exterior disease symptoms may have been judged normal even though some internal organ changes, undetectable by human eyes, may have begun. A pathological examination for characterizing samples would ideally eliminate this potential source of error.

The confusion matrix shown in table 6 summarizes the prediction errors for the strategy II optimum model. Type I error is 2% and type II error is 5.8% for normal chicken livers. For septicemic livers, type I and type II errors are 6% and 2.1%, respectively.

## CONCLUSIONS

Although comparison of models with and without offset correction preprocessing showed no obvious improvement in classification performance, the use of offset–corrected spectra is still recommended for its reduction of scattering and distance effects. A minimum number of scores is required when an acceptably high level of accuracy is desired. For instance, in the offset test, the result shows that at least 15 scores are necessary to obtain 80% accuracy. However, using too many scores will diminish classification accuracy, since the later scores will contain more noise. For example, in 1102–2498 nm region test, the results show that the accuracy obtained when using 90 input scores is lower than that when using 60 scores. Consequently, determining the minimal and optimal numbers of scores required is very problem–oriented and will vary in different cases.

Different wavelength regions were examined, and the highest classification accuracy was found using the full 400–2498 nm wavelength region, which includes both colors and chemical properties. The 400–1098 nm region also performs better than the 400–700 nm or 1102–2498 nm regions, supporting the conclusion that using regions encompassing both color and chemical data will improve classification performance.

The functional link test results showed that the number of input data points could be reduced by selecting every third data point, resulting in one–third length input spectra. The one–third model using 60 scores achieved a classification accuracy equal to the full data model using 90 scores. The functional link method itself increased the number of input data points and consequently also increased the number of scores required to maintain acceptable performance.

The iterations and momentums test for the back–propagation neural network showed that an appropriate number of training iterations is needed to avoid undertrained and overtrained situations (e.g., between 40,000 and 90,000 iterations in this study). Results from using a smaller momentum (e.g., 0.2 or 0.4) were more consistent between training and testing than the results from using a larger momentum (e.g. 0.8).

The best classification model was found with strategy II: offset correction followed by second difference (g = 31) and the use of 60 scores for neural network input data. The optimum model achieved classification accuracies of 98% for normal and 94% for septicemic. A confusion matrix analysis shows that the probabilities of Type I and Type II errors for normal livers were 2% and 5.8%, respectively, and for septicemic livers were 6% and 2.1%, respectively.

**Table 4. Comparison of the optimum model of each preprocessing strategy.**

| | Optimum Model | | Classification Accuracy (%) | |
|---|---|---|---|---|
| Strategy | Gaps | Scores | Normal | Septicemia |
| I | N/A | 90 | 92 | 86 |
| II | 31 | 60 | 98 | 94 |
| III[a] | 15 | 60 | 92 | 92 |

[a] Data points used in strategy III optimum model were every third data (see text for details).

**Table 5. Misclassified samples of the optimum model for strategy I and II.**

| Strategy | Sample Class | Training Set | Testing Set |
|---|---|---|---|
| I | Normal | 3 (N102, N104, and N149) | 4 (N109, N119, N197, and N505) |
| | Septicemic | 5 (S237, S275, S730, S734, and S738) | 7 (S224, S244, S248, S268, S701, S719, and S731) |
| II | Normal | 3 (N102, N189, and N534) | 1 (N119) |
| | Septicemic | 4 (S237, S734, S738, and S741) | 2 (S202 and S268) |

**Table 6. Confusion matrix for the optimum model of strategy II.**

| | | Predicted | | Type I |
|---|---|---|---|---|
| Actual | Total | Normal | Septicemic | error (%) |
| Normal | 50 | 49 | 1 | 2 |
| Septicemic | 50 | 3 | 47 | 6 |
| Type II error (%) | | 5.8 | 2.1 | |


### ACKNOWLEDGEMENTS

The authors would like to thank the management at Allen Family Foods for providing access to their facilities. The authors would also like to thank Dr. William R. Hruschka and Dr. Stephen R. Delwiche of ISL for their constructive comments in data analysis, and Mr. Frank Gwozdz of ISL for his technical assistance in sample collection.


## REFERENCES


Brons, A., G. Rabatel, F. Sevila, and C. Touzet. 1991. Neural network techniques to simulate human judgment on potplant quality: An artificial expert for beauty evaluation. In *Proc. Symposium of Automated Agriculture for the 21st Century,* 126–133. St. Joseph, Mich.: ASAE.

Chao, K., Y. R. Chen, H. Early, and B. Park. 1999. Color image classification systems for poultry viscera inspection. *Applied Eng. in Agric.* 15(4): 363–369.

Chen, Y. R., and D. R. Massie. 1993. Visible/near–infrared reflectance and interactance spectroscopy for detection on abnormal poultry carcasses. *Trans. ASAE* 36(3): 863–869.

Chen, Y. R., W. R. Hruschka, and H. Early. 2000. A chicken carcass inspection system using visible/near–infrared reflectance: In–plant trials. *J. Food Process Eng.* 23(2): 89–99.

Chen, Y. R., M. Nguyen, and B. Park. 1998. Neural network with principal component analysis for poultry carcass classification. *J. Food Process Eng.* 21(5): 351–367.

Chen, Y. R., K. Chao, W. R. Hruschka, and Y. Liu. 2001. Advances in sensing technologies for poultry inspection. In *Optics in Agriculture 1990–2000*. J. A. DeShazer and G. E. Meyer, eds. *SPIE Critical Review* 80: 140–181.

Cowe, I. A., and J. W. McNicol. 1985. The use of principal components in the analysis of near–infrared spectra. *Applied Spectroscopy* 39(2): 257–266.

Devaux, M. F., D. Bertrand, and G. Martin. 1986. Discrimination of bread–baking quality of wheats according to their variety by

near–infrared reflectance spectroscopy. *Cereal Chemistry* 63(2): 151–154.
Galactic Industries Corporation. 1999. GRAMS/32. Version 5.21. Salem, N.H.: Galactic Industries Corporation.
Gonzalez, R. C., and R. E. Woods. 1993. *Digital Image Processing*, 571–661. Boston, Mass.: Addison–Wesley.
Haykin, S. 1994. *Neural Networks: A Comprehensive Foundation*, 138–235. New York, N.Y.: Macmillan College Publishing.
Hruschka, W. R. 1987. Data analysis: Wavelength selection methods. In *Near–Infrared Technology in the Agricultural and Food Industries*, 35–55. P. Williams and K. Norris, eds. St. Paul, Minn.: American Association of Cereal Chemists.
Hsieh, C. L., S. F. Cheng, and T. T. Lin. 1997. Application of image texture analysis and neural network on the growth stage recognition for head cabbage seedlings. *J. Agric. Machinery* 6(2): 1–13.
Kung, S. Y. 1993. *Digital Neural Network*, 1–42. Upper Saddle River, N.J.: Prentice Hall PTR.
Næs, T., K. Kvaal, T. Isaksson, and C. Miller. 1993. Artificial neural networks in multivariate calibration. *J. Near–Infrared Spectroscopy* 1(1): 1–11.
NeuralWare. 1998. NeuralWorks Professional II/Plus. Carnegie, Pa.: NeuralWare, Inc.
Norris, K. H. 1989. Definition of NIRS analysis. In *Near–Infrared Reflectance Spectroscopy (NIRS): Analysis of Forage Quality*, 7. G. C. Martin, J. S. Shenk, and F. E. Barton II, eds. Agriculture Handbook No. 643. Beltsville, Md.: USDA Agricultural Research Service.
Osborne, B. G., T. Fearn, and P. H. Hindle. 1993. *Practical NIR Spectroscopy with Applications in Food and Beverage Analysis*, 145–199. 2nd ed. Essex, U.K.: Longman Scientific and Technology.
Park, B., Y. R. Chen, A. D. Whittaker, R. K. Miller, and D. S. Hale. 1994. Neural network modeling for beef sensory evaluation. *Trans. ASAE* 37(5): 1547–1553.
Park, B., Y. R. Chen, and R. W. Huffman. 1995. Integration of visible/NIR spectroscopy and multispectral imaging for poultry carcass inspection. *SPIE* 2345: 162–171.
Pimentel, R. A. 1979. *Morphometrics: The Multivariate Analysis of Biological Data*, 47–69. Dubuque, Iowa: Kendall/Hunt Publishing.
SAS. 1999. SAS for Windows. Release 8.0. Cary, N.C.: SAS Institute, Inc.
Thai, C. N., and R. L. Shewfelt. 1991. Modeling sensory color quality of tomato and peach: Neural networks and statistical regression. *Trans. ASAE* 34(3): 950–955.
USDA. 2000. 1998 Report of the Secretary of Agriculture to the U.S. Congress food safety and inspection service. Issued June 2000.
Zurada, J. M. 1992. *Introduction to Artificial Neural Systems*, 230–234. Eagan, Minn.: West Publishing.